Proceedings of the 8th World Congress on Mechanical, Chemical, and Material Engineering (MCM'22)
Prague, Czech Republic – July 31, 2022 - August 02, 2022
Paper No. HTFF 141
DOI: 10.11159/htff22.141

A Heat Transfer Analysis of Axial and Radial Functionally-Graded Ceramic Foams Solar Air Receivers

Assunta Andreozzi[1], Marcello Iasiello[1]
[1]Dipartimento di Ingegneria Industriale/Università degli Studi di Napoli Federico II
Piazzale Tecchio 80, Napoli, Italy
assunta.andreozzi@unina.it; marcello.iasiello@unina.it

Abstract **–** Volumetric solar receiver are promising as heat transfer devices in concentrated solar power applications because they allow to reduce heat losses at the receiver entrance when compared to more conventional tubular receivers. Among various porous materials, ceramic foams have been shown to be promising because of their extended heat transfer area and effective thermal conductivity, especially when they are manufactured by considering variable morphologies thanks to modern techniques like additive manufacturing. In this contribution, porous media numerical simulations are presented for fluid flow and heat transfer in ceramic foams receiver with different porosity functions on either axial or radial directions, and also when porosity varies on both directions. Such simulations are performed by employing Beer-Lambert law to model radiative heat transfer, and a Gaussian distribution for the incoming radiation. Results are obtained by constraining the average porosity for the different cases, showing that graded foams allow to obtain more or less similar outflow temperatures, but with reduced heat losses at the receiver entrance and also with less uniform velocity profiles to promote heat convection in some critical points of the receiver.

Keywords**:** concentrated solar power, volumetric solar air receiver, ceramic foam, numerical heat transfer, graded foams

1. Introduction

Using Concentrated Solar Power (CSP) system is nowadays one of the most promising solutions to reduce the CO_2 emissions impact on the environment. With this technology, optical concentration is employed to concentrate sunlight at a point that could be the top of a tower where a heat transfer fluid that passes through a receiver is heated to obtain high temperature energy. These receivers could be tubular or volumetric, where the latter have been showed to be more promising because of the volumetric effect that allow to reduce heat losses, achieving higher effective heat fluxes [1]. Volumetric receivers can be made in various porous materials as well as wire packs, foil arrangements or foams.

Foams are essentially porous materials with a certain regularity guaranteed by more or less periodic cell that repeat in a space [2]. These materials have been proposed to be employed as volumetric receiver to overcome honeycomb and thin silicon fibers limits in terms of practical considerations like mechanical stresses and so on [3]. Various solutions have been proposed through the years. Pritzkow [4] used a Si3N4 20 PPI foam with a special black coating by including a quartz-glass window in order to heating up air from ambient temperature to 1000 °C with pressures up to 10 bars [4]. In the SOLGATE project [5], the whole receiver is made up by three different levels modules, where the last one was made up by a ceramic foam. This module operates at the highest temperatures in order to achieve a 1000 °C air outlet temperature. After years, many mathematical model for this have been proposed. Wu et al. [6] presented both experimental and numerical results of a concentrated solar power receiver equipped with a ceramic foam, analyzing different combinations in terms of mass flow rates and foam morphology in order to achieve the best thermal performances. An analytical solution of the problem for the sake of comparisons has been presented by Sano et al. [7]. Kribus et al. [8] performed a numerical analysis with a simple model in order to investigate the configurations that maximize thermal efficiency, showing that thermal efficiency can reach up to a 90% thanks to the absorber material spectral selectivity. By placing foam layers with different morphological properties in series, Chen et al. [9] showed that layers with decreasing porosity higher air outlet temperature and lower solid inlet temperatures. A throughout parametric analysis of ceramic foams for volumetric receivers has been shown in Andreozzi et al. [10], showing that thermal efficiency can be maximized by employing foams with uniform lower cell sizes and porosities more or less equal to 0.90.

When foams are employed for heat transfer augmentation, it has been recently shown that in other fields like heat exchangers [11, 12] and thermal energy storage systems [13, 14] it is possible to increase thermal performances by employing foams with graded morphological characteristics like porosity and cell size. This has been also extensively demonstrated in ceramic foams. As already mentioned, Chen et al. [9] demonstrate that using variable morphological characteristics would increase receiver performance. Exhaustive analyses of different pore structures distributions in volumetric solar receivers have been performed by Wang and Vafai [15] and by Wang et al. [16]. By comparing increasing, decreasing and constant receivers, the authors concluded that the decreasing configuration allows to obtain an excellent performance evaluation criterion value [16]. Du et al. [17] optimized optical and radiative properties in a volumetric solar receiver designed with the modified random spherical bubbles method, obtaining a porosity distribution that maximizes the penetration depth of the solar radiation. Uniform and radial graded porous volumetric receivers are analyzed with both experimental and numerical approaches starting from CT data in [18]. The authors showed that a radial-graded porous receiver with larger pores inside might increases thermal efficiency by 4.1% with a slight decrease of a 8.6% for the flow resistance.

Based on the previous literature survey, it is evident that employing graded foams is of great potential for volumetric receivers, and there is still a lack of which could be the best combination to maximize receiver thermal performances. In this contribution, a numerical analysis of heat transfer and fluid flow in ceramic foam volumetric receiver is carried out by assuming that porosity could vary along axial, radial, or axial and radial, directions, with different porosity functions in which their average value is kept as the same. Results will be shown in terms of temperature profiles and fields in order to appreciate in which case it is possible to minimize inlet ceramic temperatures by keeping more or less constant the outlet working fluid temperature.

2. Methodology

2.1. Graded foams functions

A sketch of the investigated volumetric receiver can be found in Fig. 1. In order to investigate graded foams effects, functions with different variability but equal averaged values are here considered. By assuming that porosity would be always equal to $\varepsilon_{avg} = 0.85$, linear, exponential and a trigonometric function here assumed as the $\tan^{-1}$ function to smooth porosity variations, have been employed. For the linear and trigonometric functions, it is here assumed that porosity for $z = 0$ and $r = 0$ is equal to $\varepsilon_{max} = 0.95$, obtaining a porosity of $\varepsilon_{min} = 0.75$ at $z = L$ and $r = R$ that also correspond to $z^* = 1$ and $r^* = 1$ with $z^* = z/L$ and $r^* = r/R$. A resume of the equations that describe these variations can be find in the following.

$$\varepsilon(i) = \varepsilon_{max} - (\varepsilon_{max} - \varepsilon_{min})i^* \tag{1a}$$

$$\begin{cases} \varepsilon(i) = 0.95e^{-ki^n} \\ k(i=z) = 0.84859; k(i=r) = 1.22792 \\ n = 0.53307 \end{cases} \tag{1b}$$

$$\varepsilon(i) = \varepsilon_{avg} - \frac{tg^{-1}\left(2\frac{i - I/2}{I/2}\right)}{10tg^{-1}(2)} \tag{1c}$$

Where the symbols i, i^* and I respectively refer to cases in which z or r, z^* or r^*, and L or R, are employed, depending on whether the porosity varies along r or z

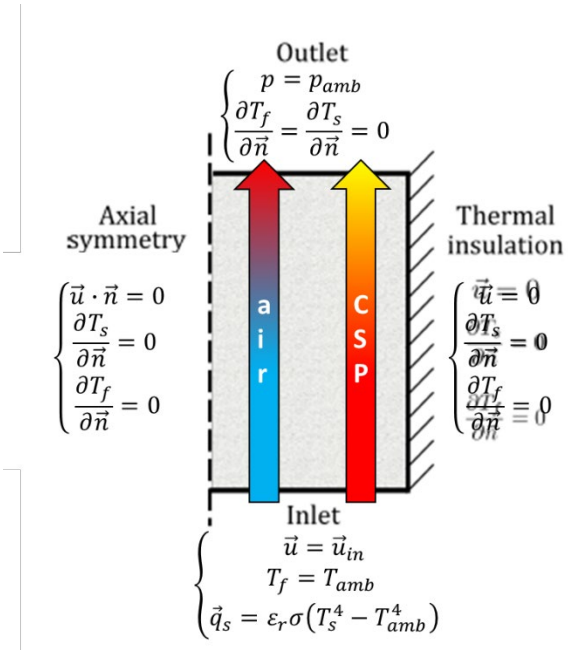

Fig. 1: Sketch of the receiver computational domain with boundary conditions

Finally, in this manuscript we've also considered the cases in which porosity varies on both axial and radial coordinate, that in practice would be possible also thanks to modern additive manufacturing techniques [18]. This mixed case is considered here by combining either linear or reverse porosity, *i. e.* $\tan^{-1}$, cases. For both cases, by constraining the average porosity at 0.80 in order to assume the same maximum and minimum porosity values, say 0.95 and 0.75, the following sets of equations can be employed

$$\begin{cases} \varepsilon_{z,lin}(z) = \varepsilon_{max} - (\varepsilon_{max} - \varepsilon_{min})z^* \\ \varepsilon_{lin}(r,z) = \dfrac{\varepsilon_{z,lin}(z) + 0.75}{2} - \dfrac{\varepsilon_{z,lin}(z) - 0.75}{2}\dfrac{r - R/2}{R/2} \end{cases} \tag{2a}$$

$$\begin{cases} \varepsilon_{z,rev}(z) = \varepsilon_{avg} - \dfrac{tg^{-1}\left(2\dfrac{z - L/2}{L/2}\right)}{10tg^{-1}(2)} \\ \varepsilon_{rev}(r,z) = \dfrac{\varepsilon_{z,rev}(z) + 0.75}{2} - \dfrac{\varepsilon_{z,rev}(z) - 0.75}{2}\dfrac{r - R/2}{R/2} \end{cases} \tag{2b}$$

2.2. Mathematical Modelling

Governing equations are essentially the same of [10] and these are briefly resumed in the following. These are written for a single-phase equivalent porous medium under the assumptions of steady state, no buoyancy and thermal dispersion effects, and under the assumption of local thermal non equilibrium. Mass, momentum, and energy equations for fluid and solid phases, respectively and by dropping the volume averaging symbols <>, are

$$\nabla \cdot (\rho\, \mathbf{u}) = 0 \tag{3a}$$

$$\frac{\rho}{\varepsilon^2}\mathbf{u}\nabla \cdot \mathbf{u} = -\nabla p + \frac{\mu}{\varepsilon}\nabla^2\mathbf{u} - \frac{\mu}{K}\mathbf{u} - \frac{\rho f}{\sqrt{K}}|\mathbf{u}|\mathbf{u} \tag{3b}$$

$$\left(\rho c_p\right)_f \mathbf{u} \cdot \nabla T_f = \nabla \cdot \left(\varepsilon k_f \nabla T_f\right) + h_v\left(T_s - T_f\right) \tag{3c}$$

$$\nabla \cdot \left[\left(\frac{1-\varepsilon}{3}\right) k_s \nabla T_s\right] - h_v\left(T_s - T_f\right) + \beta I_0 e^{-\beta z} = 0 \tag{3d}$$

Where the last term on the right side of Eq. (3d) is the radiative heat flux term modeled according with Beer-Lambert law as previously done in other works [10, 19]. The terms K, f, h_v and β are respectively the permeability, the inertial factor, the volumetric heat transfer coefficient and the extinction coefficient. The concentrated solar radiation is modeled with reference to the Gaussian distribution close to the one from Villafan-Vidales [20], $I(r) = 1.0 \cdot 10^6 e^{-2560 r^2}$, while all the thermophysical properties variable with temperature presented in this work are modeled according with [10].

In order to close governing equations, typical porous media coefficients are required. These coefficients can be obtained from the following correlations [6, 10, 21-23]

$$K = \frac{d_c^2}{1039 - 1002\varepsilon} \tag{4a}$$

$$f = \frac{0.5138\varepsilon^{-5.739}}{d_c}\sqrt{K} \tag{4b}$$

$$h_v = (32.50\varepsilon^{0.38} - 109.94\varepsilon^{1.38} + 166.65\varepsilon^{2.38} - 86.98\varepsilon^{3.38}) Re_c^{0.438} \varepsilon^{0.438} \frac{k_f}{d_c^2} \tag{4c}$$

$$\beta = \frac{3}{d_c}(1-\varepsilon) \tag{4d}$$

With dc the cell size, $Re_c = |\mathbf{u}|_{in}\, \rho\, d_c/\mu$ the cell Reynolds number. In this study we will assume d_c = 1 mm

Boundary conditions are resumed in Fig. 1 and these are essentially the same of Andreozzi et al. [10], with u_{in} = 1 m/s here and by recalling that the emissivity at the inlet section is 0.95 [6, 10]. Governing equations with appropriate boundary conditions are solved with a finite element solver. A fully coupled solver is used for all the equations, with a convergence criterion of 10^{-4} for the equation and a structured rectangular mesh. In order to find the best mesh in terms of computational effort and solution accuracy, a structured mesh with rectangular elements with uniformly spaced elements along the z direction and an element ratio of 2 along the radius. The grid independence analysis has been performed references to a case with uniform properties, say 0.80 porosity, a cell size of 1.5 m/s, a uniform solar flux of 600 kW/m^2 and an inlet velocity of 1.30 m/s. It has been shown that there is just a small improvement between a 50x50 and a 100x100 grid, concluding that a 100x100 grid would be sufficient for accurate computations here. The present model by assuming uniform properties has been already validated in Andreozzi et al. [10].

3. Results and discussion

3.1. Axial-variable porosity

Temperatures profiles for axial-variable porosity cases (Eqs. 1) are presented in Fig. 2. In all the cases, dashed curves represent fluid phases, while solid curve are referred to solid phases. With references to both phases computed at r = 0 (top-left figure), it is shown that for all cases fluid phase present a sudden increase at the beginning because of the heat that comes in from the solid phases heated by the concentrated solar power. After a certain length, these phases reach a more or less common temperatures. The slight differences and also the slight decrease for both phases along the axial direction happen because of the heat that goes along the radial direction, that is also emphasized by the fact that a Gaussian distribution is assumed for the incoming concentrated solar power. The latter observation can be applied for fluid and solid temperature profiles along both radius for $z = L$ and z = 0, where a decay along the radius can be attributed to the incoming Gaussian distribution even if velocity is zero on the boundaries, that would theoretically increase temperature here [10]. When comparing the different porosity distributions, it is shown that in all cases outlet

temperatures are more or less equal, except for the uniform distribution that presents both higher solid temperatures at the entrance and smaller fluid temperatures at the outlet. This because smaller porosities at the entrance cause higher heat transfer coefficients but also lower extinction coefficients, making the material less prone to absorb radiation. Finally, it is also shown that a reverse distribution presents higher peaks along the symmetry line because the locally higher porosity causes the solar beam to travel for longer inside the domain.

3.2. Radial-variable porosity

Results obtained from radial-variable porosity function are here introduced. Velocity fields are presented in Fig. 3 for different porosity functions. It is clear that when a uniform porosity is used, the whole velocity field approaches to a more or less uniform value as often happens for porous materials except for the walls. In all the other non-uniform cases, velocity is smaller in the core region, with a drastic increase close to the walls especially for linear and reverse functions. This trend is more pronounced here because porosity locally achieves very small values that make drag forces very high and channelling effect here very much relevant. Temperature profiles are shown in Fig. 4. It is shown that temperatures at the outlet are more or less the same on both the symmetry axis and along the radius, with slightly higher values for the reverse function on the axis. With references to the entrance section, one can notice that solid phase presents higher values if a uniform distribution is employed, where a reverse function presents the smallest value. This because the uniform distribution locally presents the smallest porosities, while on the other hand the reverse function has the highest values. As already observed before, higher porosity would cause a better solar rays penetration inside the receiver.

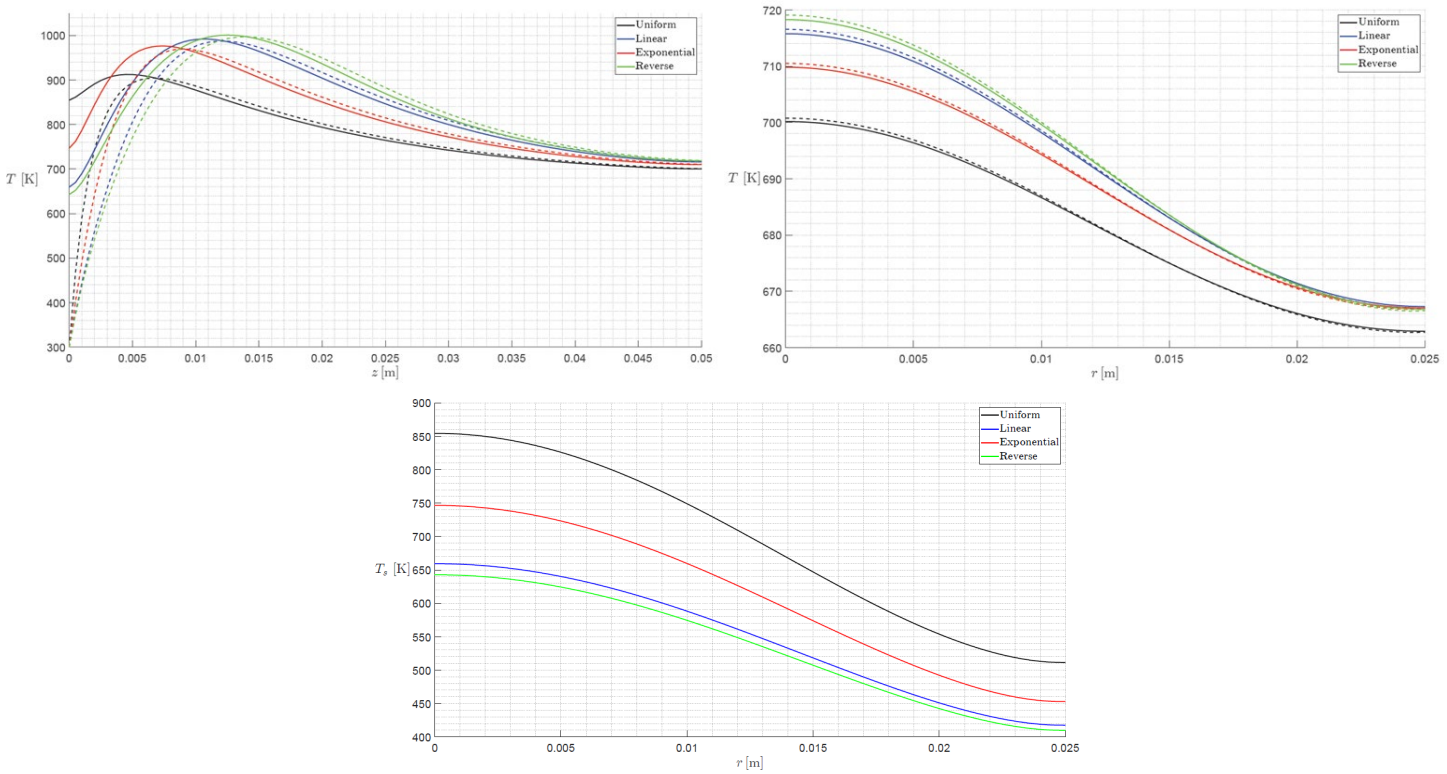

Fig. 2: Axial-variable porosity fluid and solid temperatures for r = 0 (top-left) and z = L (top-right), and solid temperature for z = 0

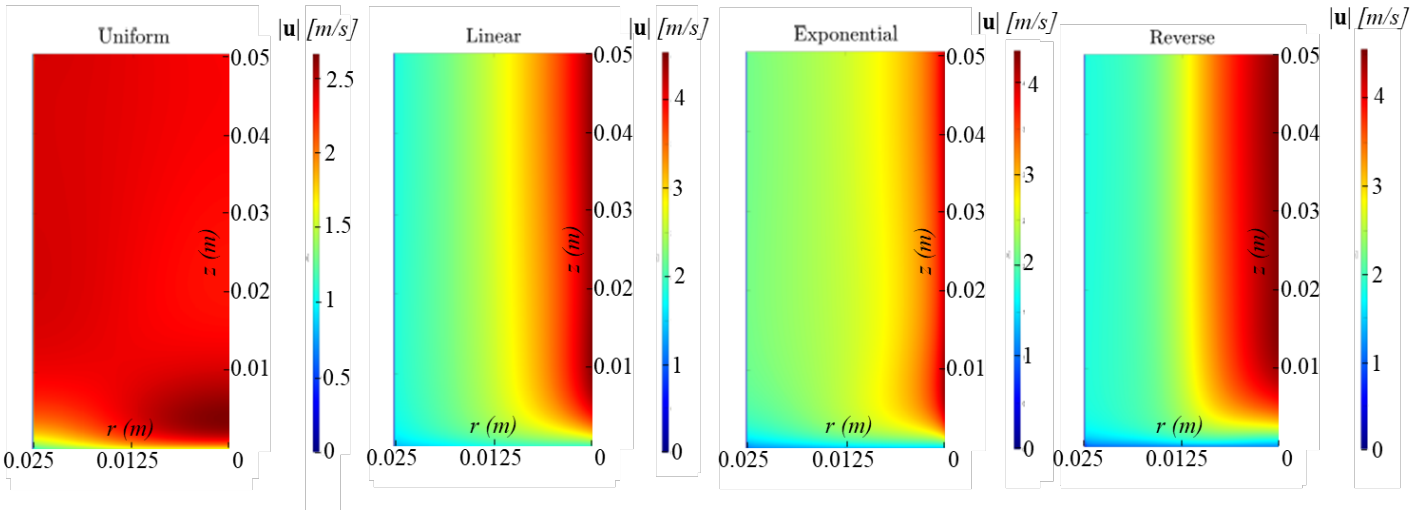

Fig. 3: Velocity fields for radial-variable porosities functions

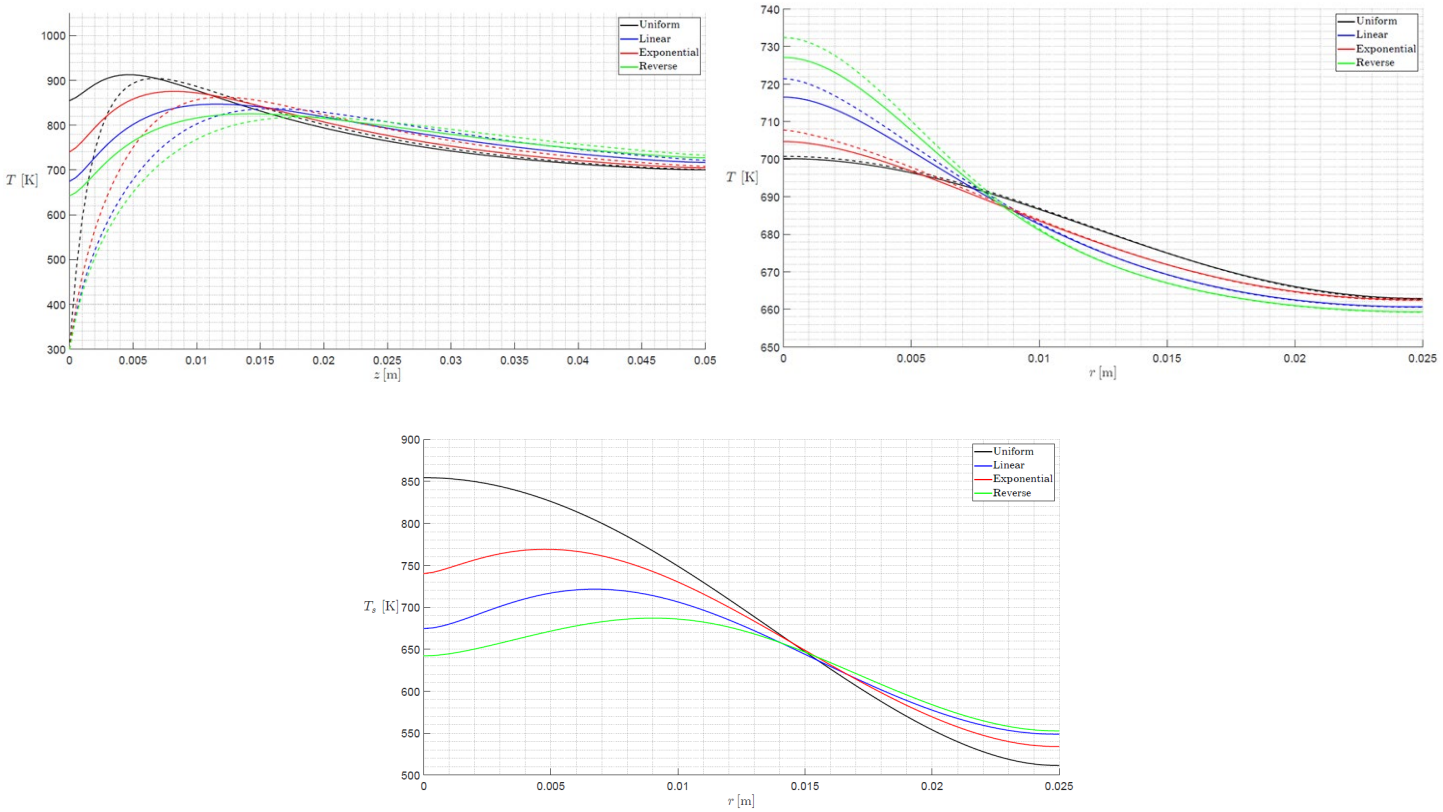

Fig. 4: Radial-variable porosity fluid and solid temperatures for $r = 0$ (top-left) and $z = L$ (top-right), and solid temperature for $z = 0$

3.3. Axial and radial-variable porosity

In this study, we've also assumed that porosity could be variable on both axial and radial coordinates, in order to see if there are some configuration that would maximize heat transfer performances thanks to this solution. Results for uniform, linear and reverse distributions are depicted in Fig. 5. It is shown that along the symmetry line, all temperatures

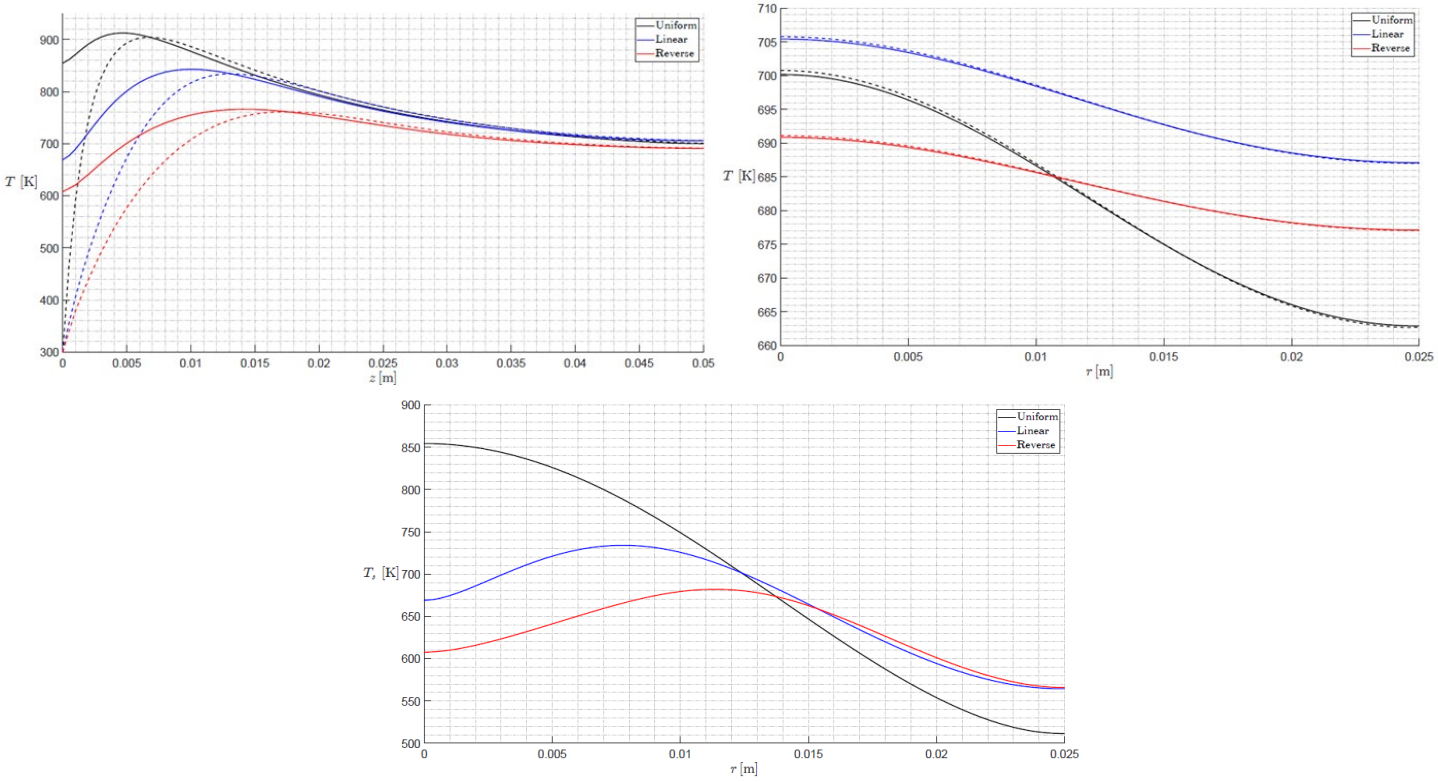

Fig. 5: Both-variable porosity fluid and solid temperatures for $r = 0$ (top-left) and $z = L$ (top-right), and solid temperature for $z = 0$

are more or less the same. With references to the radial temperature distributions for $z = L$ (top-right) and $z = 0$ (bottom), it is shown that the uniform distribution always presents the highest variability, where the highest value is achieved on the symmetry axis for $z = 0$ and the lowest one is obtained at $z = L$ for $r = R$. This means that varying the porosity across the receiver would allow to more uniform temperatures along both axial and radial directions for both solid and fluid temperatures.

4. Conclusions

In this contribution, functionally-graded ceramic foams with axial and radial variable porosity have been analyzed when applied to a volumetric solar air receiver. Various functions at constrained averaged porosity, namely linear, exponential and reverse functions, have been employed. Porous media equations with Beer-Lambert law for radiative participating media have been numerically solved by assuming a Gaussian distribution for the concentrated solar power incoming radiation. Results have been presented in terms of velocity and temperature profiles. It has been shown here that if porosity varies along either the axial or the radial direction, or on both axial and radial directions, outlet fluid temperatures are more or less the same, but a uniform distribution presents higher heat losses at the receiver entrance. Besides, a radial direction-variable porosity makes velocity profiles less uniform when compared to the uniform case, promoting heat transfer via convection where this is weaker for the uniform case. In the future, more functionally-graded functions will be analyzed to reach optimum values in terms of receiver thermal efficiency.

Acknowledgements

This work was supported by Italian Government MIUR Grant No. PRIN-2017F7KZWS.

References

[1] A. L. Avila-Marin, "Volumetric receivers in solar thermal power plants with central receiver system technology: a review," *Sol. energy*, vol. 85, no. 5, pp. 891-910, 2011.

[2] L. J. Gibson, and M. F. Ashby, *Cellular solids: structure and properties*. Cambridge, UK: Cambridge, 1997.

[3] J. M. Chavez, and C. Chaza, "Testing of a porous ceramic absorber for a volumetric air receiver," *Sol. Energ. Mater.*, vol. 24, no. 1-4, pp. 172-181, 1991.

[4] W. Pritzkow, The pressure loaded volumetric ceramic receiver 500 kW version, *DLR*, vol. 93, no. 2, 1993.

[5] P. Heller, M. Pfänder, T. Denk, F. Tellez, A. Valverde, J. Fernandez, and A. Ring, "Test and evaluation of a solar powered gas turbine system," *Sol. energy*, vol. 80, no. 10, pp. 1225-1230, 2006.

[6] Z. Wu, C. Caliot, G. Flamant, and Z. Wang, "Coupled radiation and flow modeling in ceramic foam volumetric solar air receivers," *Sol. Energy*, vol. 85, no. 9, pp. 2374-2385, 2011.

[7] Y. Sano, S. Iwase, and A. Nakayama, "A local thermal nonequilibrium analysis of silicon carbide ceramic foam as a solar volumetric receiver," *J. Sol. Energ.-T. ASME*, vol. 134, no. 2, 2012.

[8] A. Kribus, Y. Gray, M. Grijnevich, G. Mittelman, S. Mey-Cloutier, and C. Caliot, "The promise and challenge of solar volumetric absorbers," *Sol. Energy*, vol. 110, pp. 463-481, 2014.

[9] X. Chen, X. L. Xia, X. L. Meng, and X. H. Dong, "Thermal performance analysis on a volumetric solar receiver with double-layer ceramic foam," *Energ. Convers. Manage.*, vol. 97, pp. 282-289, 2015.

[10] A. Andreozzi, N. Bianco, M. Iasiello, and V. Naso, "Thermo-fluid-dynamics of a ceramic foam solar receiver: A parametric analysis," *Heat Transfer Eng.*, vol. 41, no. 12, pp. 1085-1099, 2020.

[11] M. Iasiello, N. Bianco, W. K. S. Chiu, and V. Naso, "The effects of variable porosity and cell size on the thermal performance of functionally-graded foams," *Int. J. Therm. Sci.*, vol. 160, pp. 106696, 2021.

[12] X. Chen, X. Xia, C. Sun, F. Wang, and R. Liu, "Performance evaluation of a double-pipe heat exchanger with uniform and graded metal foams," *Heat Mass Transfer*, vol. 56, no. 1, pp. 291-302, 2020.

[13] C. Hu, H. Li, D. Tang, J. Zhu, K. Wang, X. Hu, and M. Bai, "Pore-scale investigation on the heat-storage characteristics of phase change material in graded copper foam," *Appl. Therm. Eng.*, vol. 178, pp. 115609, 2020.

[14] A. Ghahremannezhad, H. Xu, M. R. Salimpour, P. Wang, and K. Vafai, "Thermal performance analysis of phase change materials (PCMs) embedded in gradient porous metal foams," *Appl. Therm. Eng.*, vol. 179, pp. 115731, 2020.

[15] P. Wang, and K. Vafai, "Modeling and analysis of an efficient porous media for a solar porous absorber with a variable pore structure," *J. Sol. Energ.-T. ASME*, vol. 139, no. 5, 2017.

[16] P. Wang, J. B. Li, K. Vafai, L. Zhao, and L. Zhou, "Thermo-fluid optimization of a solar porous absorber with a variable pore structure," *J. Sol. Energ.-T. ASME*, vol. 139, no. 5, 2017.

[17] S. Du, Q. Ren, Y. L. He, "Optical and radiative properties analysis and optimization study of the gradually-varied volumetric solar receiver," *Appl. Energ.*, vol. 207, pp. 27-35, 2017.

[18] S. Du, T. Xia, Y. L. He, Z. Y. Li, D. Li, and X. Q. Xie, "Experiment and optimization study on the radial graded porous volumetric solar receiver matching non-uniform solar flux distribution," *Appl. Energ.*, vol. 275, pp. 115343, 2020.

[19] T. Fend, P. Schwarzbözl, O. Smirnova, D. Schöllgen, and C. Jakob, "Numerical investigation of flow and heat transfer in a volumetric solar receiver," *Renew. Energ.*, vol. 60, pp. 655-661, 2013.

[20] H. I. Villafán-Vidales, S. Abanades, C. Caliot, and H. Romero-Paredes, "Heat transfer simulation in a thermochemical solar reactor based on a volumetric porous receiver," *Appl. Therm. Eng.*, vol. 31, no. 16, pp. 3377-3386, 2011.

[21] Z. Wu, C. Caliot, F. Bai, G. Flamant, Z. Wang, J. Zhang, and C. Tian, "Experimental and numerical studies of the pressure drop in ceramic foams for volumetric solar receiver applications," *Appl. Energ.*, vol. 87, pp. 504-513, 2010.

[22] K. Kamiuto, "Modeling of Composite Heat Transfer in Open-Cellular Porous Materials at High Temperatures," in *Cellular and Porous Materials: Thermal Properties Simulation and Prediction*, A. Ochsner, G. E. Murch, and M. J. S. de Lemos, Eds. Darmstadt, GER: Wiley, 2008, pp. 165-198.

[23] R. Viskanta, "Combustion and heat transfer in inert porous media," in *Handbook of porous media*, K. Vafai, Ed. Boca Raton, FL: CRC Press, 2005, pp. 625-662.